Beyond mAP: Re-evaluating and Improving Performance in Instance Segmentation with Semantic Sorting and Contrastive Flow

Rohit Jena, Lukas Zhornyak*, Nehal Doiphode*, Vivek Buch², James Gee, and Jianbo Shi

¹ University of Pennsylvania, PA, USA
² Stanford University, CA, USA
{rjena,zhornyak,lahen}@seas.upenn.edu, vpbuch@stanford.edu, gee@upenn.edu, jshi@seas.upenn.edu

Abstract. Top-down instance segmentation methods improve mAP by hedging bets on low-confidence predictions to match a ground truth. Moreover, the query-key paradigm of top-down methods leads to the instance merging problem. An excessive number of duplicate predictions leads to the (over)counting error, and the independence of category and localization branches leads to the naming error. The de-facto mAP metric doesn't capture these errors, as we show that a trivial dithering scheme can simultaneously increase mAP with hedging errors. To this end, we propose two graph-based metrics that quantifies the amount of hedging both inter- and intra-class. We conjecture the source of the hedging problem is due to feature merging and propose a) Contrastive Flow Field to encode contextual differences between instances as a supervisory signal, and b) Semantic Sorting and NMS step to suppress duplicates and incorrectly categorized prediction. Ablations show that our method encodes contextual information better than baselines, and experiments on COCO show that our method simultaneously reduces merging and hedging errors compared to state-of-the-art instance segmentation methods.

Keywords: instance segmentation, contrastive flow, metrics for segmentation

1 Introduction

Top-down instance segmentation methods suffer from two problems – (instance) merging and hedging. Merging refers to the problem of masking multiple objects that are similar as a single instance. This occurs in the query-key paradigm where a query feature generates a mask by selecting mask features. Since mask features are similar for similar instances, query features have no way to distinguish these instances, which leads to the instance merging problem. Hedging refers to the problem of predicting multiple instances of the same instance with

^{*} Equal contribution

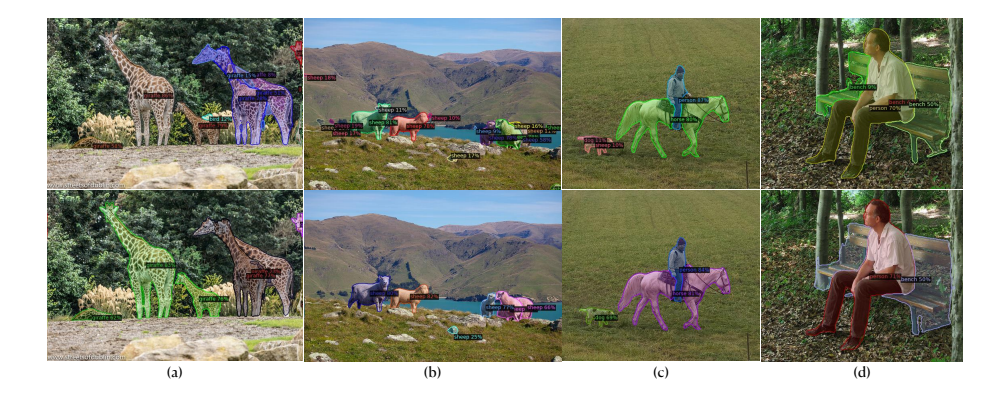


Fig. 1. Merging and Hedging on COCO-eval: Top (SOLOv2) and bottom (Ours) show instance segmentation results. Fig. (a, b) show overcounting of classes *giraffe*, *sheep* (9 giraffes, 15 sheep) as opposed to ours (6 giraffes, 6 sheep). Fig. (c) shows incorrect naming of dog as sheep in the scene. Fig. (d) shows masking error, where the bench is fragmented into its constituents.

slight variations in localization and/or class. Hedging can be intra-class (different masks for the same instance - counting) or inter-class (predicting the same mask with multiple classes - naming). A successful instance segmentation involves the integration of the category and localization branches of visual perception to solve these problems. Popular approaches are dominated by top-down methods where the network regresses a bounding box, mask, and category. Mask-RCNN [14] approaches it as a two-stage problem: localize the object, then predict the associated instance segmentation mask. SOLO [36,37] builds on an anchor-free framework and directly regresses an object segmentation using a spatial grid as a probe. More recent work based on Transformers [4] explicitly learns a query in the network memory, then refines this prediction. Despite their differences, these architectures share similar types of errors: 1) instance merging of similar objects 2) excessive hedging within and across classes. The instance merging problem occurs when the network segments two similar objects as one instance.

In analyzing why networks with widely varied designs all make these systematic forms of errors, we notice an unusual observation: one can improve mAP by substantially increasing overcounting. Specifically, we notice that mAP can be 'gamed' by hedging bets on low confidence predictions to match a ground truth. The hedging becomes more prominent as we move away from traditional NMS to more soft or implicit variations [37],[10]. Overcounting in instance segmentation can be traced to the behavior of the precision-recall (P/R) curve at its tail end (high recall range). We note that mAP discounts the tail end performance and encourages over-counting with duplicates (Fig. 2, more examples in Supplementary Material). NMS methods that are soft [37], or implicit [4],[10] tend to keep low-confidence predictions which end up in the tail end of the P/R curve, hence, increasing mAP but worsening the hedging problem. This provides

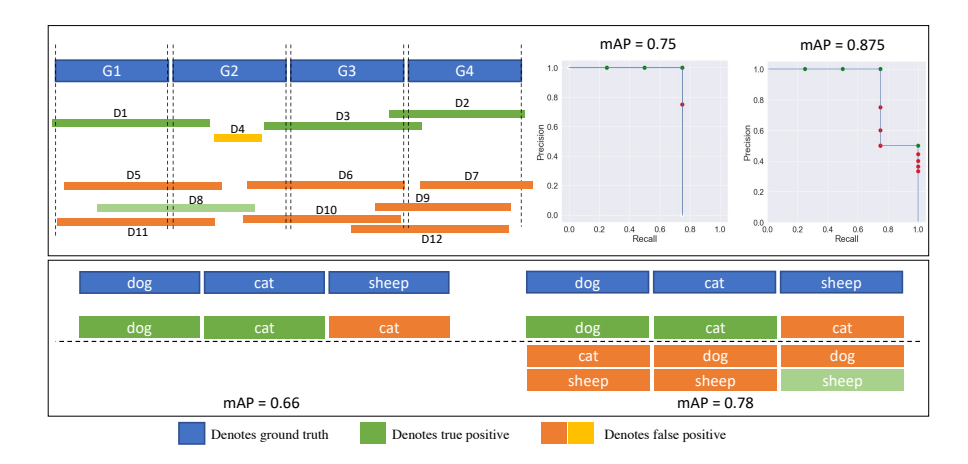


Fig. 2. Illustration of counting and naming errors that increase mAP: (a) Given ground truths G1-G4, predictions D1-D4 produce an mAP of 0.75 (D4 doesn't match with any ground truth because of low IoU). Dithering predictions D1-D4 to produce detections D5-D12 results in an accidental match of D8 with G2, leading to mAP of 0.875. (b) In the bottom example with three ground truths, a sheep is misclassified as a cat. Copying the same predictions from the left, and dithering the classification label to produce extra predictions leads to a new match, increasing mAP.

a trivial spatial dithering scheme to increase mAP by overcounting, which we notice occurs in state-of-the-art top-down instance segmentation methods due to near-identical queries. Addressing this is important for many practical counting problems such as medical applications [17], crowd detection [6], or industrial applications where counting is critical.

The current pre-NMS ranking scores are mainly predicted by an independent category branch that is often miscalibrated [13,34,18] and doesn't reflect the instance mask quality. [34] highlights that inaccurate object proposal classification can lead to a drastic performance drop in mask AP of rare classes. Moreover, implementations of modern instance segmentations allow predicting multiple classes for the same instance, exacerbating the *inter-class hedging* problem. To remove the loophole in mAP-based evaluation, we develop a new metric to quantify the amount of hedging based on graph analysis on the proposed detection/segmentation instance space and apply both within classes (counting) and across classes (naming).

The new metric allows us to explore algorithm designs that explicitly target the *hedging* errors. Top-down instance segmentation methods tend to 'pool' together instances that look similar to a single mask. This is because similar instances have similar features, and a query feature cannot distinguish between these instances. We refer to this problem as *instance merging*, and we conjecture it is a major contributor to the *hedging* problem. We notice that instance merging is similar to a problem in human vision: visual crowding [38],[31]. A human can solve this problem by shifting their gaze and attention to the area

of crowding. Inspired by this, we implement a feedback process that first uses semantic segmentation to group pixels of all similar objects into one category. To resolve this merging, we incorporate a bottom-up flow based feedback that actively pulls pixels within an instance closer and pushes those across different instances farther. We implement this by training a contrastive instance flow field, constructed as a sum of both a flow field towards the centers of each object and a flow repelling nearby instances, ensuring the nearby objects are separable. The pixel-wise contrastive instance flow is reminiscent of bottom-up grouping-based methods [29],[12],[25],[3]. However, there is a critical distinction: our flow's direction also depends on nearby crowding objects' position. This dependence helps to encode relative positions of crowding objects to separate their features and thus eliminate instance merging in the top-down prediction. Semantic segmentation can alleviate the *hedging* errors by using overlap between instance and semantic segmentation and consistency to re-rank mask proposals and use the semantic label to remove incorrectly named objects.

2 Related works

Instance segmentation Instance segmentation is often viewed as a localization task for object detection and pixel-wise classification to segment the object masks. Among such "detect then segment" strategies is FCIS [20], the first endto-end fully convolutional work that considers position-sensitive score maps as mask proposals. The score maps are then assembled to produce classification agnostic instance masks and category likelihoods. Along the same line of strategies is MaskRCNN [14], a two-stage detector that predicts masks from proposed boxes after RoIAlign operation on feature maps. Moving away from box-based object detection, SOLO[37] and CondInst[33] take an anchor-free approach and use position-sensitive query to extract object masks directly from the feature map. The use of dynamic convolution in SOLOv2, is related to transformer based approaches through works like [40], where dynamic kernels are learnt from grouped features similar to learning from queries in transformers. In SOLOv2, kernels are learnt from features on spatial grid centers. QueryInst[10], is another query based object detection framework that links mask features and objects in a one to one correspondence across multiple stages. HTC [5] is a cascade-based approach that considers semantic segmentation to refine its instance predictions.

Evaluation of Detection and Segmentation Methods The mean average precision (mAP) is a commonly used evaluation metric for objection detection, which is also adopted for image segmentation. Existing works have pointed out several shortcomings to the mAP metric for object detection. [7] show that mAP can be increased by introducing a nonsensical ranking among classes, and propose to make it truly class independent. LRP [27] highlights two major issues with mAP, i.e. 1) different detectors having different P/R curves (implying different problems) can have the same mAP, and 2) mAP is not sufficient to quantify localization. Inspired by Panoptic Segmentation, explicitly penalizes false positive and false negative detections, in addition to localization error. The TIDE

[2] framework instead identify and decomposes the error (1 - mAP) into its constituent error components to analyse where a detector is failing.

Instance Merging The top down prediction methods, where a few query points (often object centers) are responsible for predicting the whole object shape makes them prone to the instance merging problem. In contrast, bottom-up approaches focus on grouping pixels into an instance. These approaches, including Houghvoting [11,19], pixel affinity [15,23], Watershed methods [1], pixel embedding [25,24,16], can be thought of as 'flow' based: each pixel directly or indirectly learns to flow towards the object center. The flow is category agnostic, making it easier to learn and more generalizable. However, flow based methods are more error-prone than top-down methods.

Instance Separation in crowding via flow: In human vision, there exists a perception difficulty called as crowding [38,30,31], which is correlated with changeblindness. Experimentally, we noticed that many instance segmentation systems often group two similar objects nearby as one object. Very few works explicitly address the problem of instance separation in the crowded pixel space. SOLOv2 [37] adds position coordinates to convolutional mask features. However, position information is degraded in further layers. [26] point out that crowding is due to the inherent shift-invariant nature of convolution and proposes an instance coloring approach by defining a semi-convolutional operator to mix data from a convolutional network with the global location of the pixel. The embeddings regress to unconstrained representative points in each instance. This can be thought of as a center regression flow but with a semi-convolutional architecture. Other works, such as [9] propose a discriminative orientation mask to distinguish between foreground and background pixels, [3] creates a loss function to enforce cluster-and-contrast between embeddings of same and different instances.

3 Quantifying Merging and Hedging beyond mAP

3.1 Hedging Bets

Current top down-approaches suffer from a recurring problem: similar instances often produce merged instance predictions. In order to maintain a reasonable mAP, networks are thus encouraged to predict multiple predictions for each instance, each dithered slightly from each other and potentially spanning multiple classes. These, often low-confidence, duplicate predictions are the network hedging its bets in case the higher confidence prediction does not align with the ground truth. Low-confidence predictions, occupying the tail end of the precision-recall (P/R) curve, are not penalized by the mAP metric for being incorrect but are rewarded if one, by chance, matches a ground truth (see Fig. 2). This exposes a critical tradeoff in non-max supression (NMS) procedures: do we suppress duplicates but lower the recall or include them and confuse the output predictions?

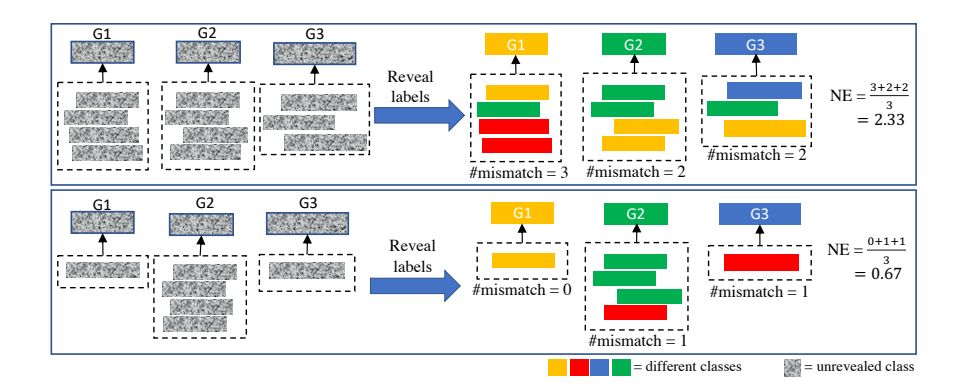


Fig. 3. Illustration of naming error: Given ground truths G1-G3, the labels of the ground truths and detections (inside dashed boxes) are hidden. Each detection is matched to a ground truth based on its localization in a class-agnostic manner. After matching, the labels are revealed, and the naming error is calculated as the average number of predictions whose labels do not match their corresponding ground truth.

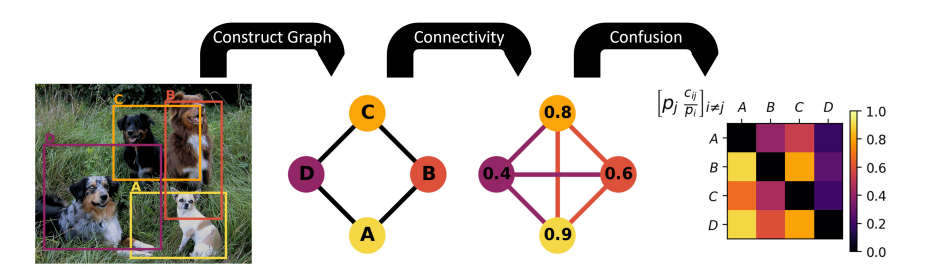


Fig. 4. Calculating duplicate confusion on a sample set of predictions as described in Section 3.2. Here, brighter colours represent larger confidences and darker colours represent smaller confidences. In this example, the duplicate confusion is 1.676.

One might question why low confidence duplicate predictions are a problem since an appropriate threshold would filter them out. In practice, confidence is often not well calibrated between classes [13] and mAP decreases monotonically with increasing thresholds, making it difficult to select a threshold that is not overly exclusionary without also including duplicates. As describe above, this is a problem that should be solved by NMS. Fundamentally, when the network makes a prediction, even a low-confidence prediction, this represents a belief by the network that there exists a unique instance at that location. By this interpretation, the low-confidence predictions are not simply unnecessary but incorrect, an error that is not captured by the mAP.

The TIDE [2] framework and the LRP both attempt to address some of the deficiency in the mAP metric. Because TIDE relies on the change in mAP to determine error, in cases such as Fig. 1, 2 it still rewards a network for hedging its predictions. In contrast, the LRP explicitly penalizes false positive and false

negative detections. Furthermore, the F1-score similarly penalizes false positives and false negatives while the boundary IoU [28] can identify when instance merging is occurring. However, none of these metrics are able to explicitly identify and penalize hedging. In order to quantify how much hedging is occurring in a set of predictions, we separate hedging into inter-class and intra-class hedging and approach both in a unified, graph-centric, approach. In doing so, we propose two new metrics, the $Naming\ Error(NE)$ and the $Duplicate\ Confusion(DC)$, to complement the existing metrics described above.

3.2 Measuring Intra-Class Hedging

To measure how much a set of predictions is exploiting dithering and duplication to increase its mAP, we design a metric which captures the relative information between the predictions for a given image. For a given IoU threshold, a graph G of the predictions within a class is constructed. The nodes of the graph are the predicted confidences and two nodes share an edge if their relative IoU is above this threshold. This graph represents, at the chosen threshold, which predictions are in the same cluster of predictions. For two nodes i and j in G, we define the connectivity between the nodes as

$$c_{ij} = \max_{t \in T_{ij}} \min_{k \in t} p_k \tag{1}$$

where T_{ij} is the set of all paths on G that connect i and j and p_k is the predicted confidence for prediction k along the path t. This represents the minimum confidence along the most connected path between two predictions. We now define the duplicate confusion at some IoU threshold u and confidence threshold v as the mean weighted sum of the connectivity of a node with all other nodes:

$$DC_{uv} = \frac{1}{n} \sum_{i}^{n} \sum_{j \neq i}^{n} p_j \frac{c_{ij}}{p_i}$$

$$\tag{2}$$

Here, n is the number of predictions with confidence at least v. For each image, the duplicate confusion DC is calculated by taking the mean of DC_{uv} across the range of IoU and confidence thresholds. This process is summarized in Fig. 4. For clarity, the DC is multiplied by 1000 in Table 1, 3.

In the above equation, the term $\frac{c_{ij}}{p_i}$ can be interpreted as a bottlenecking coefficient: for predictions i and j, how greatly is the information contained by the prediction j restricted from explaining i by the confidence of the predictions connecting i and j. Since duplicate low confidence predictions are more tolerable, this bottlenecking coefficient is weighted by the confidence of the prediction j. Consequently, the duplicate confusion DC is nondecreasing with respect to the confidence of any prediction (see Appendix). If the network is producing duplicates, the duplicate confusion can be reduced by either removing the duplicate or reducing the confidence of both predictions.

This metric can be interpreted as the confidence of a network in its own counting. This is not, however, a measure of how effectively a network can count

instances – the ground truth is not considered when calculating the metric. Neither is duplicate confusion a measure of the quality or completeness of the predictions of a network; consider, producing no predictions results in 0 duplicate confusion. Rather, the metric simply captures the amount of and uncertainty between duplicate predictions. By contrast, to increase mAP, the network is encouraged to "hedge its bets" when it is not completely certain, a behaviour heavily penalized by the duplicate confusion metric.

3.3 Measuring Inter-Class Hedging

Similar to intra-class hedging, inter-class hedging can be formulated as a connectivity problem, and penalizing the edges that connect nodes of different classes. Given the set of ground truths and predictions, we formulate the inter-class hedging as a *naming error* by penalizing hedged predictions with a different class than its corresponding ground truth.

Naming error (NE): To formulate a naming error, we need to associate ground truths with predictions in a class-agnostic way. We start by hiding the class predictions for each detection and ground truth, matching each detection with its ground truth by decreasing order of confidence of the predictions. This ensures that predictions are matched with ground truths only based on mask overlap. Note that this allows a single ground truth to be matched to potentially multiple predictions. Finally, we reveal all the labels. The naming error for a ground truth is simply the number of predictions that match this ground truth with incorrect labels. This is illustrated in Fig.3. The naming error over the dataset is the average of naming error over all ground truths. Formally, let $\{G_1 \dots G_N\}$ be the set of ground truth masks and $\{D_1 \dots D_M\}$ be the set of predictions. For each detection D_j , we define $g(D_j)$ as

$$g(D_j) = \begin{cases} \arg \max_i \text{IoU}(D_j, G_i) &, \max_i \text{IoU}(D_j, G_i) \ge 0.5\\ -1 &, \text{otherwise} \end{cases}$$
(3)

Then, the naming error is defined as

$$NE = \frac{1}{N} \sum_{i=1}^{N} \sum_{j:g(D_j)=i} \mathbb{I}[l(D_j) \neq l(G_i)]$$
 (4)

where l(.) is the function that returns the label. In the next subsection, we propose a semantic sorting module that attempts to resolve these errors.

4 Resolving merging and hedging

In this section, we propose to resolve the merging and hedging errors. Merging errors trace back to the network's inability to distinguish between instances. To resolve this, we propose a contrastive flow field that encodes the relative

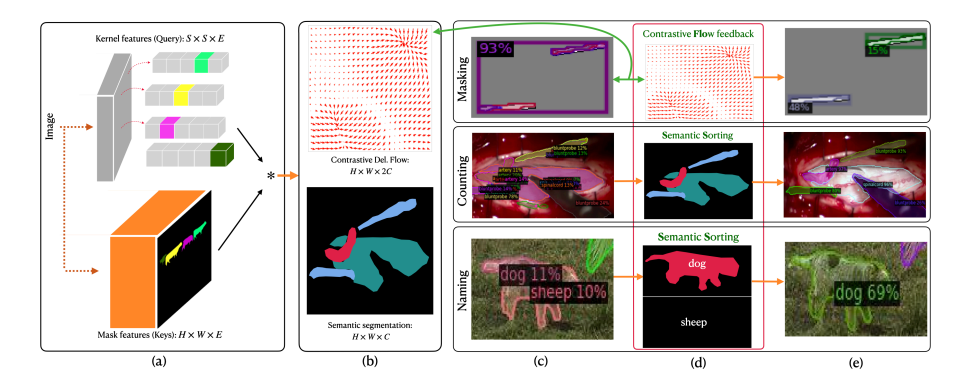


Fig. 5. Contrastive Flow and Semantic Sorting: We illustrate our approach to solving the counting, naming and masking problems. First, the mask features in SOLOv2 are used to predict a per-pixel flow and semantic segmentation. This is used for contrastive flow feedback to produce better masks, and semantic sorting tackles the counting and naming problems. In the second case, Semantic NMS prunes hedged predictions of the same object. In the third case, Semantic NMS prunes the duplicate prediction with incorrect class due to lack of a corresponding semantic mask

positioning among instances of a given class. To alleviate the hedging of the segmentation network, we propose a Semantic Sorting and NMS procedure that resolves intra-class and inter-class hedge-predictions by sequentially measuring the overlap with the semantic segmentation module.

4.1 Contrastive Delaunay Flow (CDF)

A commonly used vector flow in instance segmentation is the center flow. The idea is simple – each foreground pixel tries to regress to its instance center. However, because the center flow doesn't capture relative orientation between instances of the same class, this does not solve the problem of instance merging. For multiple instances with similar appearances, the flow vectors will likewise be similar. This doesn't resolve the ambiguity between multiple instances with similar appearance, because the flow vectors are the same for all these instances and therefore can be predicted from appearance features only. An example is illustrated in Fig.6. Moreover, the magnitude of the vector field for center flow varies significantly, especially for large objects, making it difficult to regress. This motivates the need for a flow field that captures relationships between objects and is easy to learn. The CDF addresses these problems.

The CDF consists of a unit vector at each foreground pixel, which characterizes the interactions with neighboring instances. Second, the CDF is easier to regress because the model only has to learn a direction but not a magnitude. The direction is a function of the relative location to the instance center, and the sum of repelling forces of other instances. Therefore, learning this direction amounts to learning different mask features that encode not only local appearance, but

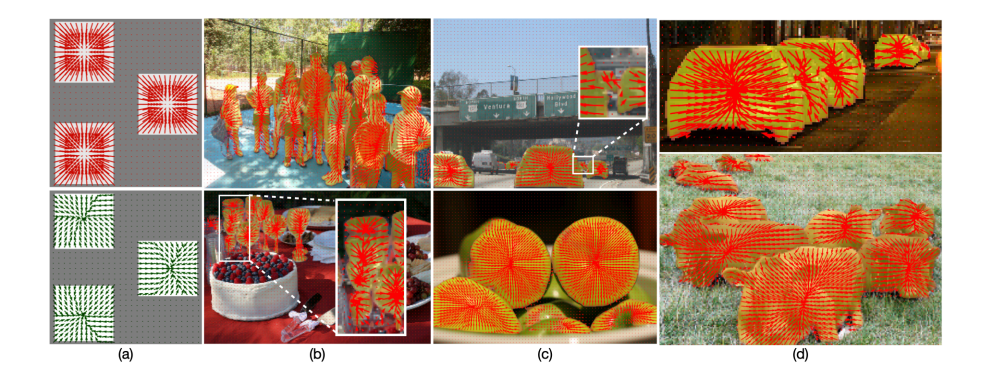


Fig. 6. Examples of Contrastive Delaunay Flow: Figure (a) shows the center flow (red) and CDF (green). The center flow for each instance is the same, which doesn't provide any contextual information. The CDF for each instance is different, providing different contexts to instances with identical appearance. Figures (b, c, d) show the learnt CDF (overlaid with learnt semantic segmentation in yellow) which exhibits contrastive repulsion in scenarios with clutter, and occlusion

also relative orientation with other instances. To incorporate both intra and inter instance context, the flow field is constructed for each class as follows:

- First, for each pixel within an instance, we initialize the vector to be a unit vector pointing towards the center of the instance. For a given instance S_k with center c_k and any pixel u such that $u \in S_k$, the vector at pixel u is initialized as $\mathbf{f}(\mathbf{u}) = \frac{\mathbf{c_k} \mathbf{u}}{\|\mathbf{c_k} \mathbf{u}\|}$.
- Second, we compute the *Delaunay triangulation* graph [8] $\mathcal{G} = \{\mathbf{V}, \mathbf{E}\}$ of all instance centers. Since calculating interactions between all pairs is both expensive and difficult to learn, the Delaunay triangulation allows us to efficiently encode the relationships and relative orientations between objects. For each edge (S_i, S_j) in the graph \mathcal{G} , we compute a unit repulsive force $\mathbf{f_{ij}} = \frac{\mathbf{c_i} \mathbf{c_j}}{\|\mathbf{c_i} \mathbf{c_j}\|}$ and $\mathbf{f_{ji}} = -\mathbf{f_{ij}}$. These forces are then added to pixels in instances S_i and S_j respectively. To break symmetry, we add these forces only to pixels that are "facing" the neighboring instance. Finally, the vector field is normalized to be of unit norm.

Instead of using the flow field in a bottom up manner during inference, we use the supervision from the CDF to amplify differences in mask features during training, therefore correcting the instances in the top-down mask prediction process directly. This is similar to [26,9,35] where bottom-up grouping supervision is used to improve top-down predictions, however, our choice of flow provides both discriminative and structural guidance in doing so.

4.2 Semantic Sorting

To detect and remove hedge-predictions, we need a 'verification' mechanism for each predicted instance along both spatial and class dimensions. To this end, we

Table 1. Ablation study: We perform ablations on the semantic segmentation and CDF modules on coco-minitrain dataset. Adding the CDF and SS branches leads to better counting and naming. Variants running with SemanticNMS have considerably better DC, LRP, and F1, indicating better resolution of the counting problem. SemanticNMS also leads to a lower naming error. M: Matrix NMS, m: Mask NMS, S: Semantic NMS

Semseg	CDF	NMS	Counting			Ma	sking	Naming	A DA	T DD
			DC↓	$LRP_{FP} \downarrow$	F1↑	b-IoU↑	$LRP_{Loc} \!\!\downarrow$	NE↓	AP↑	LRP↓
×	X	Matrix	55.6	92.61	18.46	43.0	22.43	1.93	26.34	95.88
×	×	Mask	16.0	88.52	29.82	42.9	22.13	1.56	26.16	42.77
$\overline{\checkmark}$	×	Matrix	62.0	92.55	27.49	43.4	22.50	1.95	27.26	95.85
\checkmark	X	Mask	19.2	88.29	29.50	43.6	22.20	1.56	27.08	93.42
$\overline{\checkmark}$	×	Sem	2.5	82.48	34.03	44.1	22.66	1.20	25.34	90.95
$\overline{\checkmark}$	$\overline{\checkmark}$	Matrix	63.5	91.99	17.87	44.1	22.44	1.68	28.15	95.56
$\overline{\checkmark}$	$\overline{\checkmark}$	Mask	17.4	86.76	30.82	44.3	22.12	1.33	27.94	92.60
~	$\overline{\checkmark}$	Sem	2.3	79.29	36.05	44.7	21.84	0.98	26.37	89.25
			Indicates best result			Ir	dicates seco	ılt		

add semantic segmentation as a lightweight module built on top of the instance mask features. This serves two purposes. First, it helps to re-rank instances based on their degree of 'agreement' with the corresponding class of the semantic mask. This prevents instances with poor masks but high confidence from suppressing high-quality predictions. Second, it prevents hedging by allowing only those instances which have a significant 'overlap' with the semantic mask, subtracting the corresponding instance from the semantic map. Duplicate predictions have little overlap with the remaining semantic mask and will be removed.

Calibrated pre-NMS re-ranking Since the confidence predictions are unreliable, we use semantic segmentation as an additional signal to calibrate the quality of an instance prediction. Moreover, once we have a notion of 'agreement' between an instance and a semantic mask, it is easy to rank instances in order of their mask quality. We re-rank instances based on the following factors: (i) **Precision:** An instance which has a high precision w.r.t. the semantic mask is a good instance. (ii) IoU: For instances with similar class scores and precision, we would prefer smaller instances, to avoid merged instances from appearing first in the sorted order. (iii) Category score: This score is predicted by the category branch. A detailed pseudocode can be found in the Supplementary Material.

Semantic NMS Once we have a pre-NMS scoring that is more indicative of the quality of the segmentation, we propose a Semantic NMS that uses the semantic mask for suppression. In order of confidence, if an instance has a minimum precision threshold with the semantic mask, the instance is preserved and is subtracted from the semantic mask. Otherwise, the instance is suppressed (discarded). This ensures that each instance has enough agreement with respect to the semantic mask to be preserved. A duplicate instance with a lower con-

CDF	XY	AP50	F10.5	LRP	LRPLoc		*		/			0.8
×	X	96.87	0.47	79.65	16.55		·					0.6
X	✓	96.90	0.46	79.87	16.06							0.4
✓	Х	98.01	0.99	33.46	15.87	1				7		0.2
1	✓	98.01	0.99	33.37	15.75	(a) Original	lmage	(b) SOLOV	7	(c) Our	· //	0.0

Table 2. Ablation on CDF vs CoordConv (denoted as XY) in the synthetic dataset. Note that SOLOv2 uses CoordConv by default, but removing CoordConv doesn't affect performance. Adding CDF, however, results in a huge shift in both localization and counting performance. Figure on the right shows an example of instance merging, where Fig(b) and (c) show the similarity of the *mask features* with the mask feature of the pixel marked \times in Fig(a). Our method amplifies mask feature differences based on their contrasting Delaunay neighbors, leading to predictions shown in Fig(c)

fidence would not satisfy the precision threshold since the previous instance is subtracted from the semantic mask, leaving no overlap for this duplicate mask. Only one iteration over each instance mask ensures an O(n) time complexity.

5 Experiments

Implementation. Given an input image $I \in \mathbb{R}^{3 \times H \times W}$, the FPN backbone generates a list of $[F \times \frac{H}{k} \times \frac{W}{k}]$ feature maps(where k is pyramid level), which feed into the category, kernel and mask feature prediction branch to give $\mathbb{R}^{S_k \times S_k \times C}$, $\mathbb{R}^{S_k \times S_k \times E}$ and $\mathbb{R}^{H' \times W' \times E}$ dimensional output respectively, where $H', W' = \frac{H}{4}, \frac{W}{4}, C$: semantic classes, S_k : grid size, E: feature maps. Then, one 1×1 convolution and two 1×1 convolutions with GroupNorm[39] and ReLU are performed on $mask\ features$ to output vector flow $\in \mathbb{R}^{H' \times W' \times 2C}$ and semantic segmentation $\in \mathbb{R}^{H' \times W' \times C}$ predictions respectively.

5.1 Ablation study on instance separation

Synthetic dataset To isolate the merging problem, we construct a synthetic dataset of 20 identical nails that are placed randomly in the image. Each image is of size 394×394 and the locations of the nails are sampled from a truncated random normal distribution around the image center. The training and validation set consist of 2000 and 500 images respectively. The main challenges of this dataset are instance clutter and a lack of distinct appearance between two instances which can lead to instance merging.

Performance with CDF The ablation is shown in Table 2. Even in a simple scenario, SOLOv2 suffers from severe overcounting and instance merging problems. Note that explicit coordinates (CoordConv) do not improve AP, F1 and LRP indicating no resolution of hedging and masking. Adding CDF improves all results significantly. The CDF forces different instances to learn different mask features in order to predict a different flow for each instance, where the flow is

Table 3. Instance Segmentation on coco-val-2017: Top and bottom rows are with ResNet-50-FPN and ResNet-101-FPN backbone respectively. Our method outperforms SOLOv2 on the F1 score by a factor of 2.08, showing that we explicitly reduce the counting problem. We perform substantially better at CC, F1, boundary IOU, LRP, and NE, showing that we tackle counting, masking, and naming errors in our method

M-41 J		Counting		Mas	sking	Naming	A DA	LRP↓
Method	DC↓	$LRP_{FP}{\downarrow}$	F1↑	b-IoU↑	$LRP_{Loc} \!\! \downarrow$	$NE\downarrow$	AP↑	
ResNet-50-FPN								
Mask-RCNN	76.1	80.3	38.4	49.6	20.6	0.63	37.2	88.4
SOLOv2	64.1	90.4	20.8	49.8	20.6	1.13	37.6	94.4
HTC	62.3	93.9	23.3	49.9	20.4	2.19	37.4	96.3
QueryInst (100 queries)	14.9	95.1	17.1	16.9	20.6	2.78	37.5	97.1
CondInst	144.1	88.1	30.7	50.2	20.5	1.35	37.4	92.9
Ours (Matrix NMS)	62.5	91.0	21.2	49.9	20.5	1.50	36.9	94.7
Ours	2.0	78.1	43.3	50.5	20.1	0.94	34.7	87.6
			ResNe	t-101-FPN				
Mask-RCNN	62.6	77.5	41.7	50.4	20.0	0.56	38.6	86.6
SOLOv2	63.1	89.5	21.6	50.8	20.0	1.05	39.0	93.7
HTC	48.3	92.7	26.4	51.1	20.0	1.98	39.6	95.5
QueryInst (100 queries)	10.9	94.7	19.9	17.0	19.6	2.64	41.0	96.7
CondInst	126.2	86.1	33.5	50.9	20.2	1.17	38.5	91.6
Ours (Matrix NMS)	66.7	89.5	21.3	50.8	20.1	1.05	39.4	93.8
Ours	1.9	70.6	45.9	51.4	19.2	0.57	37.4	83.4
Ir	dicates	best result	Ir	Indicates second best result				

a function of its Delaunay triangulation. An example is shown in Tab. 2. Note that nails that have similar local appearance have a very high cosine-similarity to each other in the mask feature space. Therefore, a kernel feature when convolved with this mask feature ends up masking both instances. Our method explicitly reduces mask feature similarity in order to be able to predict the CDF, which is a function of the relative positions of the neighbors. This results in a drastic reduction of merged instance prediction compared to the baseline.

5.2 Ablation on coco-minitrain

Next, we investigate the effectiveness of CDF and semantic sorting in improving hedging (intra and inter class) and merging. Therefore, we ablate on the CDF (\checkmark/\checkmark) , semantic segmentation module (\checkmark/\checkmark) , and NMS type (Matrix/mask/ Semantic). We perform ablations on the coco-minitrain [32] dataset. We use coco-minitrain instead of the COCO-train-2017 set owing to similar data statistics as the full training set and to reduce the cost of running ablations. All hyperparameters used for SOLOv2 follow the experimental setup of [37]. The results are in **Table 1**. For a given NMS method (mask/matrix/semantic), adding CDF increases mAP and masking performance over its counterpart without CDF, showing the effectiveness of the CDF in providing reliable context. The

boundary IoU metric shows that true positives now have better contour quality compared to the baseline, and LRP_{Loc} shows that CDF helps in better localization leading to better masks. Meanwhile, using semantic NMS provide at least a 86.8 % decrease in the duplicate confusion and a 15.4 % increase in the F1 score compared to Matrix and Mask NMS. Using Semantic NMS leads to a much better DC, F1, LRP_{FP}, and NE showing better resolution of both inter-class and intra-class hedge-predictions.

5.3 Result on COCO-val-2017

We run our full method on the COCO [21] training set. Results are shown in Table 3. To contrast the effect of Semantic NMS, we also compare our method but with MatrixNMS. Methods like QueryInst [10] use a fixed number of queries (e.g. 100) and produce predictions for each query without performing any NMS. The tail end behavior of these queries is therefore undefined. This leads to it having the highest mAP values, but the poorest performance in terms of F1, bloU (owing to memorization of templates), LRP and NE (due to FPs from other classes). Higher LRP_{FP} indicates more intra-class hedging, while higher DC indicates strong connectivity among the hedged predictions. However, since the predictions produced by QueryInst communicate with each other and selfseparate, QueryInst manages to achieve the second best performance in terms of duplicate confusion. In general, the behavior of different algorithms is performant along different dimensions, like HTC [5] being better at localization and MaskRCNN [14] being better at F1 and LRP. Intra-class hedging error is high in other state-of-the-art models because the classification and segmentation branches operate independently and can output multiple classes for the same instance. MaskRCNN uses the same RoIAligned boxes for classification and segmentation, essentially entangling their representations. Furthermore, MaskR-CNN chooses one category for each prediction, leading to less dithering among classes. Although MaskRCNN uses NMS, it has high DC, which means the connectivity of its hedges is very high, although the actual quantity of hedges is low (as denoted by F1 and LRP_{FP}). Our method is based on SOLOv2, which has independent category and mask branches. However, our semantic sorting and NMS helps close the gap between category and instance predictions, resolving the naming problem, and we perform closely to MaskRCNN in naming.

6 Conclusion

We highlight two important problems in instance segmentation, namely, merging and hedging. We highlight the ways in which intra and inter-class hedging errors can increase mAP, and propose metrics that isolate these errors. To address merging, we learn a contrastive flow that encourages each pixel to learn a flow dependent on the relative positions of the instances around it. To address hedging, we propose a semantic sorting mechanism that re-ranks instances and

prunes duplicates, leading to better resolution of both inter and intra-class hedging. Empirically, we show that many top-down instance segmentation methods suffer from these three errors even if they have high mAP. Experiments on the COCO dataset shows better resolution of the merging and hedging errors by our method compared to other SOTA algorithms.

References

- Bai, M., Urtasun, R.: Deep watershed transform for instance segmentation. In: Proceedings of the IEEE Conference on Computer Vision and Pattern Recognition. pp. 5221–5229 (2017) 5
- Bolya, D., Foley, S., Hays, J., Hoffman, J.: Tide: A general toolbox for identifying object detection errors. In: European Conference on Computer Vision. pp. 558–573. Springer (2020) 5, 6
- Brabandere, B.D., Neven, D., Gool, L.V.: Semantic instance segmentation with a discriminative loss function. CoRR abs/1708.02551 (2017), http://arxiv.org/ abs/1708.02551 4, 5
- Carion, N., Massa, F., Synnaeve, G., Usunier, N., Kirillov, A., Zagoruyko, S.: Endto-end object detection with transformers. In: European Conference on Computer Vision. pp. 213–229. Springer (2020) 2
- Chen, K., Pang, J., Wang, J., Xiong, Y., Li, X., Sun, S., Feng, W., Liu, Z., Shi, J., Ouyang, W., et al.: Hybrid task cascade for instance segmentation. In: Proceedings of the IEEE/CVF Conference on Computer Vision and Pattern Recognition. pp. 4974–4983 (2019) 4, 14
- Chu, X., Zheng, A., Zhang, X., Sun, J.: Detection in crowded scenes: One proposal, multiple predictions. In: Proceedings of the IEEE/CVF Conference on Computer Vision and Pattern Recognition. pp. 12214–12223 (2020) 3
- 7. Dave, A., Dollár, P., Ramanan, D., Kirillov, A., Girshick, R.: Evaluating large-vocabulary object detectors: The devil is in the details. arXiv preprint arXiv:2102.01066 (2021) 4
- 8. Delaunay, B., et al.: Sur la sphere vide 10
- 9. Du, W., Xiang, Z., Chen, S., Qiao, C., Chen, Y., Bai, T.: Real-time instance segmentation with discriminative orientation maps. In: Proceedings of the IEEE/CVF International Conference on Computer Vision. pp. 7314–7323 (2021) 5, 10
- Fang, Y., Yang, S., Wang, X., Li, Y., Fang, C., Shan, Y., Feng, B., Liu, W.: Instances as queries. In: Proceedings of the IEEE/CVF International Conference on Computer Vision. pp. 6910–6919 (2021) 2, 4, 14
- Gall, J., Lempitsky, V.: Class-specific hough forests for object detection. In: 2009
 IEEE Conference on Computer Vision and Pattern Recognition. pp. 1022–1029
 (2009). https://doi.org/10.1109/CVPR.2009.5206740
- Gao, N., Shan, Y., Wang, Y., Zhao, X., Yu, Y., Yang, M., Huang, K.: Ssap: Single-shot instance segmentation with affinity pyramid. In: Proceedings of the IEEE/CVF International Conference on Computer Vision. pp. 642–651 (2019) 4
- 13. Guo, C., Pleiss, G., Sun, Y., Weinberger, K.Q.: On calibration of modern neural networks. In: International Conference on Machine Learning. pp. 1321–1330. PMLR (2017) 3, 6
- 14. He, K., Gkioxari, G., Dollár, P., Girshick, R.: Mask r-cnn. In: Proceedings of the IEEE international conference on computer vision. pp. 2961–2969 (2017) 2, 4, 14

- Ke, T.W., Hwang, J.J., Liu, Z., Yu, S.X.: Adaptive affinity fields for semantic segmentation. In: Proceedings of the European Conference on Computer Vision (ECCV). pp. 587–602 (2018) 5
- Kong, S., Fowlkes, C.C.: Recurrent pixel embedding for instance grouping. In: Proceedings of the IEEE Conference on Computer Vision and Pattern Recognition. pp. 9018–9028 (2018) 5
- 17. Kumar, N., Verma, R., Anand, D., et al.: A multi-organ nucleus segmentation challenge. IEEE Transactions on Medical Imaging **39**(5), 1380–1391 (2020). https://doi.org/10.1109/TMI.2019.2947628 **3**
- 18. Kuppers, F., Kronenberger, J., Shantia, A., Haselhoff, A.: Multivariate confidence calibration for object detection. In: Proceedings of the IEEE/CVF Conference on Computer Vision and Pattern Recognition Workshops. pp. 326–327 (2020) 3
- Leibe, B., Leonardis, A., Schiele, B.: Combined object categorization and segmentation with an implicit shape model. In: Workshop on statistical learning in computer vision, ECCV. vol. 2, p. 7 (2004) 5
- Li, Y., Qi, H., Dai, J., Ji, X., Wei, Y.: Fully convolutional instance-aware semantic segmentation. In: Proceedings of the IEEE conference on computer vision and pattern recognition. pp. 2359–2367 (2017) 4
- Lin, T.Y., Maire, M., Belongie, S., Hays, J., Perona, P., Ramanan, D., Dollár, P., Zitnick, C.L.: Microsoft coco: Common objects in context. In: European conference on computer vision. pp. 740–755. Springer (2014) 14
- Liu, S., Jia, J., Fidler, S., Urtasun, R.: Sgn: Sequential grouping networks for instance segmentation. In: Proceedings of the IEEE International Conference on Computer Vision. pp. 3496–3504 (2017) 4
- Maire, M., Narihira, T., Yu, S.X.: Affinity cnn: Learning pixel-centric pairwise relations for figure/ground embedding. In: Proceedings of the IEEE Conference on Computer Vision and Pattern Recognition. pp. 174–182 (2016) 5
- 24. Maire, M., Yu, S.X., Perona, P.: Object detection and segmentation from joint embedding of parts and pixels. In: 2011 International Conference on Computer Vision. pp. 2142–2149 (2011). https://doi.org/10.1109/ICCV.2011.6126490 5
- 25. Newell, A., Huang, Z., Deng, J.: Associative embedding: End-to-end learning for joint detection and grouping. In: Proceedings of the 31st International Conference on Neural Information Processing Systems. p. 2274–2284. NIPS'17 (2017) 4, 5
- Novotny, D., Albanie, S., Larlus, D., Vedaldi, A.: Semi-convolutional operators for instance segmentation. In: Proceedings of the European Conference on Computer Vision (ECCV). pp. 86–102 (2018) 5, 10
- 27. Oksuz, K., Cam, B.C., Kalkan, S., Akbas, E.: One metric to measure them all: Localisation recall precision (lrp) for evaluating visual detection tasks. IEEE Transactions on Pattern Analysis and Machine Intelligence (2021) 4
- 28. Perazzi, F., Pont-Tuset, J., McWilliams, B., Van Gool, L., Gross, M., Sorkine-Hornung, A.: A benchmark dataset and evaluation methodology for video object segmentation. In: 2016 IEEE Conference on Computer Vision and Pattern Recognition (CVPR). pp. 724–732 (2016). https://doi.org/10.1109/CVPR.2016.85 7
- 29. Pont-Tuset, J., Arbelaez, P., Barron, J.T., Marques, F., Malik, J.: Multiscale combinatorial grouping for image segmentation and object proposal generation. IEEE transactions on pattern analysis and machine intelligence **39**(1), 128–140 (2016) 4
- 30. Rosenholtz, R.: Demystifying visual awareness: Peripheral encoding plus limited decision complexity resolve the paradox of rich visual experience and curious perceptual failures. Attention, Perception, & Psychophysics pp. 1–25 (2020) 5
- 31. Rosenholtz, R., Yu, D., Keshvari, S.: Challenges to pooling models of crowding: Implications for visual mechanisms. Journal of vision 19(7), 15–15 (2019) 3, 5

- 32. Samet, N., Hicsonmez, S., Akbas, E.: Houghnet: Integrating near and long-range evidence for bottom-up object detection. In: European Conference on Computer Vision (ECCV) (2020) 13
- 33. Tian, Z., Shen, C., Chen, H.: Conditional convolutions for instance segmentation. In: Computer Vision–ECCV 2020: 16th European Conference, Glasgow, UK, August 23–28, 2020, Proceedings, Part I 16. pp. 282–298. Springer (2020) 4
- 34. Wang, T., Li, Y., Kang, B., Li, J., Liew, J., Tang, S., Hoi, S., Feng, J.: The devil is in classification: A simple framework for long-tail instance segmentation. In: European Conference on computer vision. pp. 728–744. Springer (2020) 3
- 35. Wang, W., Zhou, T., Yu, F., Dai, J., Konukoglu, E., Van Gool, L.: Exploring cross-image pixel contrast for semantic segmentation. In: Proceedings of the IEEE/CVF International Conference on Computer Vision (ICCV) (2021) 10
- 36. Wang, X., Kong, T., Shen, C., Jiang, Y., Li, L.: Solo: Segmenting objects by locations. In: European Conference on Computer Vision. pp. 649–665. Springer (2020) 2
- 37. Wang, X., Zhang, R., Kong, T., Li, L., Shen, C.: Solov2: Dynamic and fast instance segmentation. In: Larochelle, H., Ranzato, M., Hadsell, R., Balcan, M.F., Lin, H. (eds.) Advances in Neural Information Processing Systems. vol. 33, pp. 17721–17732. Curran Associates, Inc. (2020), https://proceedings.neurips.cc/paper/2020/file/cd3afef9b8b89558cd56638c3631868a-Paper.pdf 2, 4, 5, 13
- 38. Wijntjes, M.W., Rosenholtz, R.: Context mitigates crowding: Peripheral object recognition in real-world images. Cognition 180, 158–164 (2018) 3, 5
- 39. Wu, Y., He, K.: Group normalization. In: Proceedings of the European conference on computer vision (ECCV). pp. 3–19 (2018) 12
- 40. Zhang, W., Pang, J., Chen, K., Loy, C.C.: K-net: Towards unified image segmentation. Advances in Neural Information Processing Systems **34** (2021) **4**

Supplementary Material

A Behaviour of Duplicate Confusion

For any two predictions a and b and associated confidences p_a and p_b where the connectivity between them is not restricted by the confidence of an intermediary prediction (i.e. $c_{ab} = \min(p_a, p_b)$), the duplicate confusion (DC) associated with these predictions is nondecreasing in p_a and p_b . Suppose, without loss of generality, that $p_a > p_b$:

$$DC = \frac{1}{2} \sum_{i}^{2} \sum_{j \neq i}^{2} p_{j} \frac{c_{ij}}{p_{i}}$$

$$= \frac{1}{2} \left(p_{a} \frac{\min(p_{a}, p_{b})}{p_{b}} + p_{b} \frac{\min(p_{a}, p_{b})}{p_{a}} \right)$$

$$= \frac{1}{2} \left(p_{a} + \frac{p_{b}^{2}}{p_{a}} \right)$$

The derivative of the DC with respect to p_a and p_b is thus

$$\frac{\partial DC}{\partial p_a} = \frac{1}{2} \left(1 - \frac{p_b^2}{p_a^2} \right)$$
$$\frac{\partial DC}{\partial p_b} = \frac{1}{2} \left(p_a + \frac{p_b}{p_a} \right)$$

which are positive on the ranges $[p_b, 1]$ and $(0, p_b]$, respectively. Since we assumed that $p_a > p_b$, we thus conclude that the DC for any two predictions with unrestricted connectivity is nondecreasing in p_a and p_b .

If, instead, there is some other prediction c that bottlenecks the connectivity between a, b such that $c_{ab} = p_v$ (and thus $p_c \le p_a$ and $p_c \le p_b$), we can decompose the DC into three components: the DC between a and b, a and c, and b and c respectively:

$$DC = \frac{p_c}{3} \left(\frac{p_a}{p_b} + \frac{p_b}{p_a} \right) + \frac{1}{3} \left(p_a + \frac{p_c^2}{p_a} \right) + \frac{1}{3} \left(p_b + \frac{p_c^2}{p_b} \right)$$

While the above is nondecreasing in p_c , this is no longer the case for p_a and p_b . Specifically, the first term (associated with the DC between a and b) in the above equation is nonincreasing in p_a and p_b . Since c_{ab} is not dependent on p_a or p_b , a and b become increasingly bottlenecked by p_c as p_a and p_b increase. As a and b become increasingly unable to fully explain each other, their DC decrease. At the same time, c becomes increasingly explainable by a and b and thus the DC increases. In combination, the total DC decrease with respect to p_a and p_b when one is approximately equal to p_c and increases when they are larger.

For more complicated connectivity graphs, the behaviour of the duplicate confusion follows a similar pattern to that described above.

B Implementation of Contrastive Delaunay Flow and Semantic Sorting

In Section 4.1, we motivate and propose the use of Contrastive Delaunay Flow, and showed its effectiveness in amplifying feature differences between similar instances. A pseudocode for the method is presented in Alg. 1.

Algorithm 1: Pseudocode for constructing CDF for class c, given set of ground truth instances S_k with centers t_k and category c

```
Data: \{S_k,\}_{k=1...N}, \{t_k\}_{k=1...N}, N
Result: Flow \mathbf{f}_c characterizing CDF for class c
// Initialize with center flow
for k = 1 ... N do
 | \mathbf{f}_c[u] \leftarrow \frac{t_k - u}{\|t_k - u\|} , \forall u \in S_k
// No graph in case of single instance
if N == 1 then
 \mid return \mathbf{f}_c
end
 // Construct graph as set of directed edges
if N == 2 then
 \mathcal{G} \leftarrow \{\{0,1\},\{1,0\}\}
else
 \mid \mathcal{G} \leftarrow \text{Delaunay}(t_1, t_2 \dots t_N)
end
// Construct flow
for (i,j) \in \mathcal{G} do
      \hat{f}_{ij} \leftarrow \frac{t_i - t_j}{\|t_i - t_j\|}
    \mathbf{f}_c[u] \leftarrow \mathbf{f}_c[u] + \mathbb{I}((t_i - u)^T \hat{f}_{ij} > 0) \hat{f}_{ij}, \forall u \in S_i
\begin{array}{c} \mathbf{f}_c[u] = \frac{\mathbf{f}_c[u]}{\|\mathbf{f}_c[u]\| + \epsilon} \\ \text{return } \mathbf{f}_c \end{array}
```

Moreover, Semantic Sorting and NMS are also shown to be effective methods for resolving both intra-class hedging (counting) and inter-class hedging (naming) errors. A pseudocode of Semantic Sorting and NMS is presented in Alg. 2.

C Separation of instance features using CDF

In this section, we show more qualitative examples of similarity in the *mask* features leading to merged predictions in the synthetic dataset (Tab. 2). The CDF represents an explicit output that is contextual, and leads to better instance merging resolution, which tackles the merging problem due to redundant query features, and lack of distinguishing features. Examples are shown in Fig. 7.

Algorithm 2: Pseudocode for semantic sorting and NMS, given instances S_k with category c_k and confidence p_k , and semantic masks M

```
Data: \{S_k, c_k, p_k\}_{k=1...N}, \{M_c\}_{c=1...C}
Result: Boolean array keep indicating preservation of instances
for k = 1 \dots N do
    pr \leftarrow \operatorname{precision}(S_k, M_{c_k});
    iou \leftarrow \text{computeIoU}(S_k, M_{c_k});
    p_k \leftarrow p_k + pr + (1 - iou);
end
(S, c, p) = \operatorname{sort}(S, c, p); // sort by decreasing p
keep \leftarrow [True] \times N;
for k = 1 \dots N do
     overlap \leftarrow \operatorname{precision}(S_k, M_{c_k});
     if overlap \ge thr then
          keep_k = True;
          M_{c_k} = M_{c_k} \backslash S_k
     else
          keep_k = False
     end
\quad \mathbf{end} \quad
```

D Shortcoming of AP for measuring hedging errors

In this section, we explore some real examples from the COCO validation dataset in terms of hedging errors and its effect on mAP. This shortcoming occurs due to low-confidence false-positives that are not explicitly pruned in a post-processing step like NMS (or thresholding low-confidence predictions after a 'soft' NMS). These low-confidence predictions accumulate in the tail end of the Precision-Recall curve, and do not negatively contribute to the mAP metric. Some examples are shown in Fig. 8. This is also reflected in Tab. 1, 3 where hedging improves mAP, but at the cost of worsening all other errors (F1-score, LRP, NE, DC). More qualitative results are shown in Fig. 9, 10, 11.

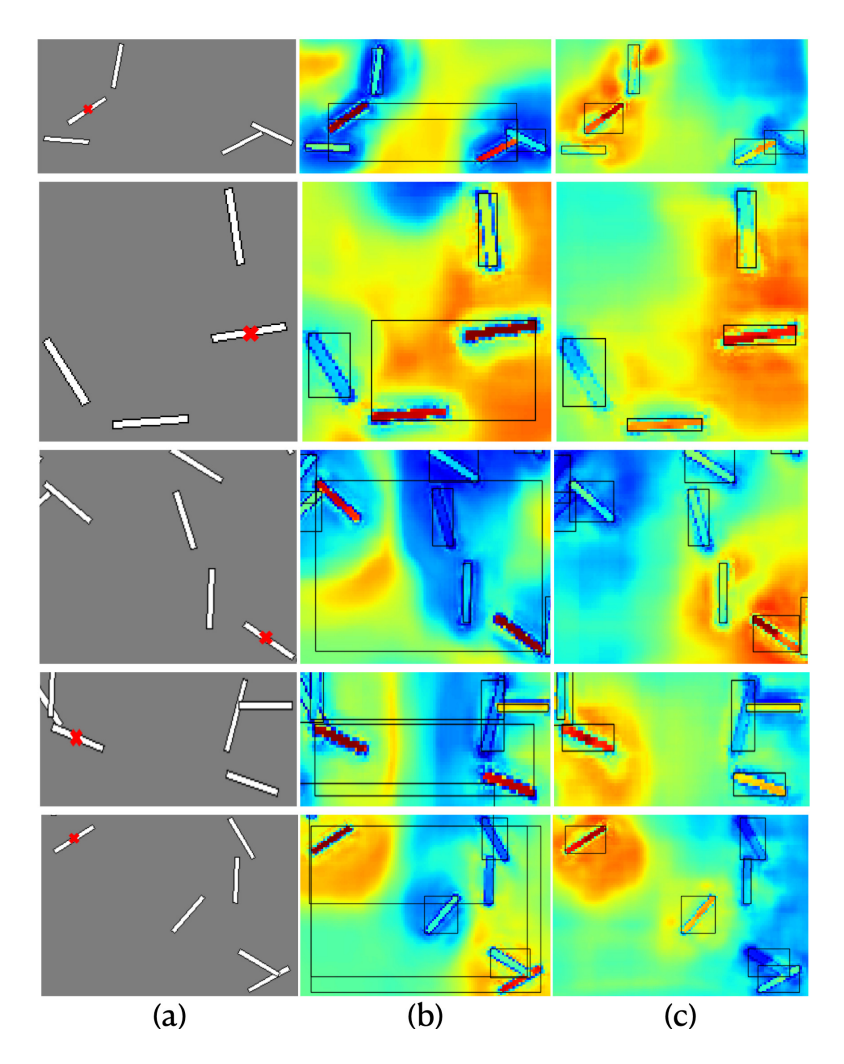


Fig. 7. More examples of instance merging problem in Synthetic dataset Each row shows examples of mask feature similarity in SOLOv2 and our method. Fig.(a) shows input image patches with similar objects. Fig.(b) shows the pixel-wise cosine similarity of the mask features with the mask feature of the pixel marked \times in Fig.(a) along with predictions (shown as bounding boxes). Note that instance merging is rampant, among instances that have similar orientation, regardless of their spatial proximity or instances around them. Fig.(c) shows our method with CDF which leads to amplification of difference in features (due to contrasting Delaunay neighbors) leading to resolution of merged predictions



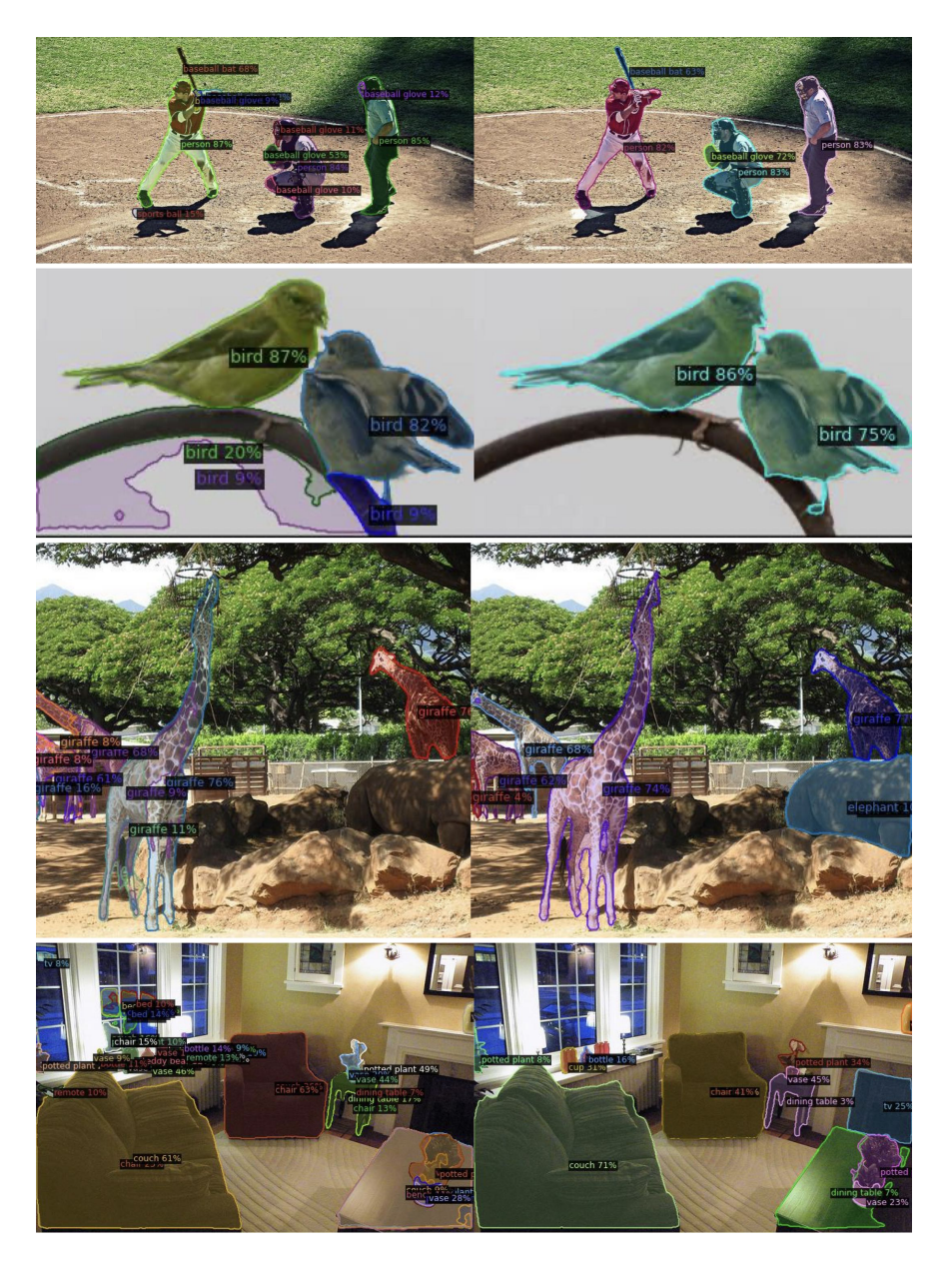
Fig. 8. Shortcoming of AP in resolving the *hedging problem*: (a) shows the prediction of SOLOv2 model with Matrix NMS, (b) shows the corresponding P/R curve. (c) shows the prediction with the same network but with Mask NMS, (d) shows the corresponding P/R curve. Note that despite having severe hedging (overcounting) in the first case, the AP scores are the same for both cases. However, they exhibit drastically different qualitative behavior, showing that AP is not an adequate metric for evaluating the *hedging problem*



 ${\bf Fig.\,9.\,\,Qualitative\,\,comparison\,\,on\,\,COCO\text{-}val\text{-}2017\,\,dataset}\colon \rm Images\,\,on\,\,left\,\,are\,\,predictions\,\,made\,\,by\,\,SOLOv2,\,\,images\,\,on\,\,right\,\,are\,\,predictions\,\,by\,\,our\,\,model\,\,with\,\,CDF,\,\,Semantic\,\,Sorting\,\,and\,\,Semantic\,\,NMS}$



 ${\bf Fig.\,10.\,\,Qualitative\,\,comparison\,\,on\,\,COCO\text{-}val\text{-}2017\,\,dataset}\colon \rm Images\,\,on\,\,left\,\,are\,\,predictions\,\,made\,\,by\,\,SOLOv2,\,\,images\,\,on\,\,right\,\,are\,\,predictions\,\,by\,\,our\,\,model\,\,with\,\,CDF,\,\,Semantic\,\,Sorting\,\,and\,\,Semantic\,\,NMS}$



 ${\bf Fig.\,11.\,\,Qualitative\,\,comparison\,\,on\,\,COCO\text{-}val\text{-}2017\,\,dataset}\colon \rm Images\,\,on\,\,left\,\,are\,\,predictions\,\,made\,\,by\,\,SOLOv2,\,images\,\,on\,\,right\,\,are\,\,predictions\,\,by\,\,our\,\,model\,\,with\,\,CDF,\,\,Semantic\,\,Sorting\,\,and\,\,Semantic\,\,NMS}$